Applied Radiation and Isotopes 143 (2019) 72–78

Contents lists available at ScienceDirect

Applied Radiation and Isotopes

journal homepage: www.elsevier.com/locate/apradiso

Measurement of ^{232}Th and ^{238}U neutron capture cross-sections in the energy range 5–17 MeV

S. Mukherjee[a,*], Vibha Vansola[a], Siddharth Parashari[a], R. Makwana[a], N.L. Singh[a], S.V. Suryanarayana[b], S.C. Sharma[b], B.K. Nayak[b], H. Naik[c]

[a] *Department of Physics, Faculty of Science, The M. S. University of Baroda, Vadodara 390020, India*
[b] *Nuclear Physics Division, Bhabha Atomic Research Centre, Mumbai 400085, India*
[c] *Radiochemistry Division, Bhabha Atomic Research Centre, Mumbai 400085, India*

HIGHLIGHTS

- The cross-sections for Th and U (n,γ) reactions were measured within the neutron energies 5–17 MeV.
- Covariance analysis has been performed to calculate the uncertainties in the measured cross-sections.
- The measured data would be useful for the ADSs and the future reactor development.

ARTICLE INFO

Keywords:
^{232}Th(n, γ) and ^{238}U(n, γ) reactions
^{7}Li(p, n) reaction neutron source
Capture cross-section activation technique
Off-line γ-ray spectrometry
Covariance matrices
TALYS-1.9

ABSTRACT

The neutron capture cross sections of ^{232}Th and ^{238}U at the average neutron energies of 5.08 ± 0.17, 8.96 ± 0.77, 12.47 ± 0.83, and 16.63 ± 0.95 MeV have been measured by using the activation technique and off-line γ-ray spectroscopy. The ^{232}Th and ^{238}U were irradiated with neutrons produced from the ^{7}Li(p, n) reaction using the proton energies of 7, 11, 15 and 18.8 MeV from the 14UD BARC-TIFR Pelletron facility in Mumbai, India. Detailed covariance analysis was also performed to evaluate the uncertainties in the measured cross-sections. The excitation function of the ^{232}Th(n, γ) and ^{238}U(n, γ) reactions were calculated using the theoretical model code TALYS-1.9. The experimental and theoretical results from the present work were compared with the ENDF/B-VII-1 and JENDL-4.0 nuclear data libraries and were found to be in good agreement.

1. Introduction

Natural thorium has only one isotope i.e., ^{232}Th with 100% isotopic abundance, whereas natural uranium has three isotopes, namely ^{234}U, ^{235}U and ^{238}U with isotopic abundances 0.006%, 0.71% and 99.3% respectively. ^{232}Th and ^{238}U being the fertile materials need to be acted upon to convert them into fissile materials to use as fuel materials of a nuclear reactor. This is one of the new concepts worldwide for the nuclear power generation, and major efforts are going on in this direction. Among them, accelerator driven sub-critical systems (ADSs) (Rubbia et al., 1995; Bowman, 1998), compact and high-temperature fast reactors (IAEA, 2002) and advanced heavy water reactor (AHWR) are the most important for power production. Besides power production, nuclear waste disposal is also an important challenge to be tackled to ensure the future sustainable growth of nuclear power. It can be achieved in ADSs, where incineration of the long-lived actinides and transmutation of the long-lived fission products can be done besides power production. The fuel cycle based on thorium (Th) can address both these issues owing to some favorable neutronics and material characteristics (IAEA, 2002). ^{232}Th is a fertile host and has to be converted into ^{233}U, a fissile isotope. Similarly, ^{238}U needs to be converted into fissile isotope ^{239}Pu. The thermal neutron capture cross section in ^{238}U is 2.47 times more than that in ^{232}Th. Thus, uranium offers greater competition for the capture of the neutrons and lower losses to structural and other parasitic materials leading to an improvement in the conversion of ^{238}U to ^{239}Pu.

* Corresponding author.
E-mail address: sk.mukherjee-phy@msubaroda.ac.in (S. Mukherjee).

https://doi.org/10.1016/j.apradiso.2018.10.013
Received 12 May 2018; Received in revised form 6 September 2018; Accepted 9 October 2018
Available online 22 October 2018
0969-8043/

Fertile

$$ {}^{232}_{90}Th + n \rightarrow {}^{233}_{90}Th(22\ min) \xrightarrow{\beta-decay} {}^{233}_{91}Pa(27\ d) \xrightarrow{\beta-decay} {}^{233}_{92}U $$

$$ {}^{238}_{92}U + n \rightarrow {}^{239}_{92}U(24\ min) \xrightarrow{\beta-decay} {}^{239}_{93}Np(2.3\ d) \xrightarrow{\beta-decay} {}^{239}_{94}Pu $$

Fissile

The decay scheme given above clears that the production of fissile nucleus ^{239}Pu depends on the ^{238}U(n, γ) reaction cross-section and the production of fissile nucleus ^{233}U depends on the ^{232}Th(n, γ) reaction cross-section. In ADSs, the energy of neutrons is much higher than the conventional reactors. Thus, the ^{232}Th(n, γ) and ^{238}U(n, γ) reaction cross-sections at higher neutron energies offer a substantial impact on the performance and safety assessment of ADSs and fast reactors. From India's perspective, which has abundant reserves of thorium, ADSs is relevant as one can also exploit its potential to design hybrid reactor systems that can produce nuclear power with the use of thorium as the primary fuel (Rubbia et al., 1995; Bowman, 1998). The fast neutrons produced in all the above types of reactors will irradiate the materials of the reactor and will cause different reactions. Thus, for the design of different types of reactors, the nuclear data such as reaction and fission cross-sections of structural materials, cladding materials and fuel elements with medium to fast neutron energies are very much valuable.

Literature survey on the fission and reaction cross section measurements related to Th and U fuel cycles show that exhaustive experimental works have been carried out in the region of low energy neutrons, which are available in the EXFOR (EXFOR, 2014) compilation. However, most of the nuclear data in the neutron-induced fission of actinides from the compilation are based on average neutron spectrum of the reactor. The experimental data in the medium to high mono-energetic (5–20 MeV) neutron-induced fission and reaction of actinides, have immense importance for the design of advanced reactors and ADSs are limited (EXFOR, 2014). In the ^{232}Th(n, γ) reaction, the cross-section within the neutron energies from thermal to 2.45 MeV and at 14.6 MeV available are primarily based on the physical measurements and activation technique (Perkin et al., 1958; Karamanis et al., 2001). However, the measured data at the neutron energy of 14.6 MeV based on DT neutron source by (Perkin et al., 1958) is significantly higher than the expected trend. Except for the experimental ^{232}Th(n, γ) reaction cross-section at the neutron energy of 14.6 MeV (Perkin et al., 1958), rest of the data within the neutron energies of 3–17.28 MeV are measured by various authors (Naik et al., 2011, 2015; Prajapati et al., 2012; Mukerji et al., 2012; Crasta et al., 2012; Bhike et al., 2012). In spite of all these, there is no data available between the neutron energies of 3.7–5.9 MeV. In the case of ^{238}U(n, γ) reaction, sufficient cross-section data are available in literature (Perkin et al., 1958; Linenberger et al., 1944; Linenberger et al., 1946; Leipunskiy et al., 1958; Barry et al., 1964; Drake et al., 1971; Panitkin and Tolstikov, 1972a, 1972b; Poenitz, 1975; HuangZheng-De et al., 1980; Naik et al., 2012) within a wide range of neutron energy. However, below neutron energy of 8 MeV, the data of early years by (Linenberger et al., 1946; Leipunskiy et al., 1958; Barry et al., 1964; Panitkin and Tolstikov, 1972a, 1972b) are significantly higher than the theoretical predictions. Similarly, above the neutron energy of 14 MeV, the ^{238}U(n, γ) reaction, cross-sections data by (Perkin et al., 1958) and (Panitkin and Tolstikov, 1972a, 1972b) are significantly higher than the theoretical values. These observations were made by comparing the similar data within the neutron energies of 2.45–17.3 MeV (Barry et al., 1964; Poenitz, 1975; HuangZheng-De et al., 1980; Naik et al., 2012; Mukerji et al., 2013; Crasta et al., 2014; Mulik et al., 2014)

The present work is aimed at further investigating the above aspects by experimental measurements of the neutron capture cross sections for ^{232}Th and ^{238}U in the neutron energy range of 5–17 MeV. Since there were various sources which can produce large uncertainties in the present measurement. Therefore, a detailed co-variance analysis was carried out to study how error propagates from various quantities into the final measured cross-section values. The present study also describes the excitation functions of ^{232}Th(n, γ) and ^{238}U(n, γ) reactions calculated using the theoretical model code TALYS-1.9 (Koning et al., 2015). Both the experimental and theoretical results from the present work were compared with the evaluated data of the ENDF/B-VII-1 (ENDF/B-VII.1, 2011) and JENDL-4.0 (Shibata et al., 2011) nuclear data libraries.

2. Experimental details

The present experiment was carried out using the 14 UD Bhabha Atomic Research Center-Tata Institute of Fundamental Research (BARC-TIFR) Pelletron Facility in Mumbai, India (Naik et al., 2011, 2012; Prajapati et al., 2012; Makwana et al., 2017). The high energy quasi mono-energetic neutron beam was obtained from the ^{7}Li(p, n) reaction by using the proton beams of different energies from the main line at a 6-meter height above the analyzing magnet of the Pelletron facility. The energy spread for the proton beam at this port was 50–90 keV. Further, a collimator of 6 mm diameter has been used in front of the target. At this port, the terminal voltage was regulated by generating voltage mode (GVM) using terminal potential stabilizer. The generated quasi mono-energetic neutrons were used to irradiate the solid targets of the fertile elements (^{232}Th and ^{238}U), which have immense importance for the development of advanced reactors and ADSs. A natural lithium foil of thickness 8.0 mg/cm^2 sandwiched between two tantalum foils of different thickness has been used for the production of neutrons via the ^{7}Li(p, n) reaction. The front tantalum foil facing the proton beam was kept with the thickness of 3.7 mg/cm^2. On the other hand, a Ta foil of thickness 4.12 mg/cm^2 was used at the back side to reduce the energy of the proton beam further. The degradation of the proton beam in the Ta-Li-ta stack was calculated by the SRIM code (Ziegler, 2004). The effective neutron energies were calculated using the proton energy values at the center of the Li target. Behind the Ta-Li-Ta stack, the natural ^{232}Th and ^{238}U metal foil samples of thickness 0.025 mm and area 1 × 1 cm^2 were used for the irradiation. The samples were wrapped with a 0.025 mm thick aluminum foil (purity > 99.99%). The aluminum wrapper was used to stop and to collect the fission products recoiling out from the surface of the samples and to avoid the radioactive contamination of other samples and surrounding materials. The Al wrapped ^{232}Th and ^{238}U metal foils were mounted at a distance of 2.1 cm from the location of the Ta-Li-Ta stack. A schematic diagram of irradiation set up is shown in Fig. 1.

Different sets of samples were made for each irradiation at different neutron energies. The Ta-Li-Ta stack along with the Al wrapped ^{232}Th

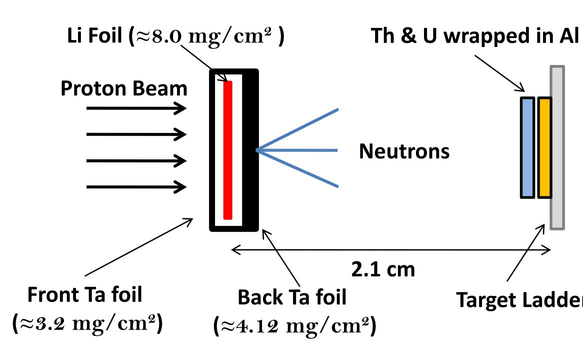

Fig. 1. Experimental arrangement showing the neutron production using the ^{7}Li(p, n) reaction.

Table 1
Details of the sample weights with their respective irradiation properties.

	Irradiation −1	Irradiation-2	Irradiation-3	Irradiation-4
Proton energy (MeV)	18.8	7.0	15.0	11.0
Irradiation time (h:min)	5:00	11:15	7:00	16:05
Beam current (nA)	140	100	135	150
Thorium weights (g)	0.1955	0.1911	0.1907	0.1905
Uranium weights (g)	0.3127	0.2995	0.2884	0.4473

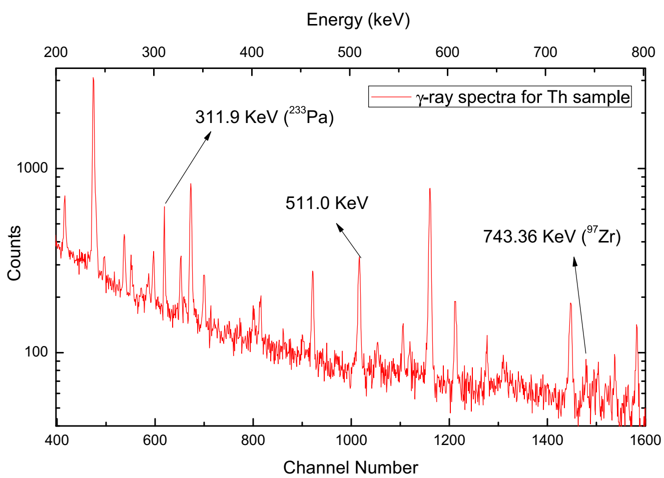

Fig. 2. Typical γ-ray spectrum from the irradiated sample of ^{232}Th at 18.8 MeV.

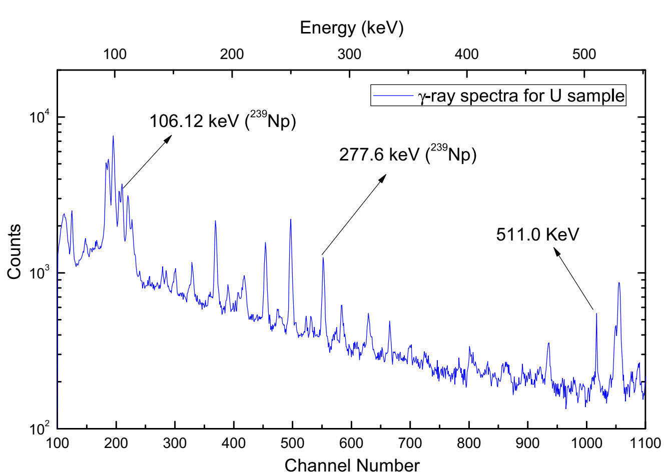

Fig. 3. Typical γ-ray spectrum from the irradiated sample of ^{238}U at 18.8 MeV.

and ^{238}U metal foil were irradiated with the proton energies (E_p) of 7, 11, 15 and 18.8 MeV respectively. The irradiation details for each sample is given in Table 1. After the irradiation, the samples were cooled for some time. Then the irradiated targets of Th and U along with Al wrapper were mounted on the different perspex plates and were taken for γ-ray spectrometry.

The γ-rays of fission/reaction products from the irradiated Th and U samples were counted by the energy and efficiency calibrated 80 cm^3 HPGe detector coupled with a PC-based 4 K channel analyzer. The resolution of the detector system during the counting was measured as 2.0 keV at 1332 keV of ^{60}Co. The counting dead time of the detector was kept less than 2% by placing the irradiated Th, and U samples at a suitable distance from the detector head to avoid the pileup effects. The energy and the efficiency calibration of the detector system were done using the standard ^{152}Eu multi γ-ray source. A similar detector geometry was used for the counting of all the irradiated samples. The γ-ray counting of the irradiated Th and U samples was repeated over an

Table 2
Fission and reaction products, half-lives, decay modes and prominent γ-ray energies with branching intensities (abundances) (NuDat). The γ-ray energies marked with bold letters were used in the calculations.

Nuclide	Half-life	Decay mode	E_γ (keV)	I_γ (%)
$^{97}_{40}Zr$	16.749 ± 0.008 h	β⁻(100%)	355.40	2.09
			507.64	5.03
			743.36	**93.09**
			1147.97	2.62
$^{233}_{91}Pa$	26.975 ± 0.013 d	β⁻(100%)	**311.9**	38.5
$^{239}_{93}Np$	2.356 ± 0.003 d	β⁻(100%)	**106.12**	**25.34**
			209.75	3.363
			228.18	10.73
			277.6	**14.51**

extended period according to the half-life of the irradiated samples to reduce the statistical error. Typical gamma-ray spectra recorded from the irradiated Th and U samples are shown in Figs. 2 and 3.

3. Data analysis

3.1. Calculation of neutron energy, flux and ^{232}Th(n, γ) and ^{238}U(n, γ) reaction cross-sections

To estimate an accurate cross-section, it is necessary to measure the neutron flux incident on the target. In the present experiment, we have used ^{232}Th and ^{238}U as target isotopes. The fission reaction ^{232}Th(n, f) was considered as a flux monitor in the present experiment for the measurement of the neutron flux incident on the target. We have followed the same procedure to measure the flux as discussed in our earlier publication (Makwana et al., 2017). The neutron spectra which were used in the estimation of flux were also taken from our previous work (Makwana et al., 2017). The spectroscopic data used for the flux and reaction cross-section measurements were taken from NuDat and are given in Table 2. In the fission of ^{232}Th, the ^{97}Zr isotope has been produced as a product, which has a half-life of 16.749 ± 0.008 h (NuDat). The produced ^{97}Zr isotope can be estimated by measuring 743.36 keV (NuDat) gamma peak area. The fission yields of ^{97}Zr are known (Naik et al., 2016; Mukerji et al., 2014). Hence, one can estimate the neutron flux using neutron activation analysis (NAA) technique. The fission yield values for the ^{97}Zr isotope have been taken from the literature (Naik et al., 2016; Mukerji et al., 2014) and are given in Tables 3 and 4. The spectrum-averaged cross sections for the fission reaction were calculated using the recent data available in the ENDF/B-VII.1 database. The neutron flux (Φ) incident on the target was estimated by using the following equation,

$$\Phi = \frac{A_{obs}\frac{CL}{LT}\lambda}{NY\sigma_f I_\gamma \varepsilon(1 - e^{-\lambda T_i})e^{-\lambda T_c}(1 - e^{-\lambda CL})} \quad (1)$$

Where N is the number of target atoms, Y is ya ield of the fission products (Naik et al., 2016; Mukerji et al., 2014) and σ_f is the spectrum averaged cross-section of the fission reaction. The fission cross-sections are available for wide range neutron energies in literature, which is compiled in the EXFOR database (EXFOR, 2014). λ is the decay constant ($\lambda = \ln 2/T_{1/2}$) of the reaction product of interest with a half-life as

Table 3
The ^{232}Th(n, γ) reaction cross-section at different neutron energy.

Neutron energy (MeV)	^{97}Zr Fission yields (%)	Spectrum averaged cross-section for Th monitor (mb)	Flux (n/cm^2.sec)	$^{232}_{90}Th(n,\gamma)$ reaction cross section (mb)			
				Present work (mb)	TALYS-1.9 (mb)	ENDF (mb)	JENDL (mb)
5.08 ± 0.17	4.639 ± 0.42 (Naik et al., 2016)	99.0	1.06E+06	2.26 ± 0.37	7.82	2.607	2.827
8.96 ± 0.77	4.838 ± 0.35 (Naik et al., 2016)	220.0	4.2E+06	1.46 ± 0.21	1.07	0.881	1.204
12.47 ± 0.83	4.672 ± 0.33 (Naik et al., 2016)	270.0	1.11E+07	1.33 ± 0.26	1.53	1.155	1.379
16.63 ± 0.95	3.41 ± 0.15 (Mukerji et al., 2014)	342.0	1.11E+07	0.78 ± 0.12	0.754	0.356	0.642

$T_{1/2}$. I_γ is the branching intensity of the 743.36 keV γ-line of ^{97}Zr and ε is its detection efficiency. CL, LT, Ti, and *T*c are the real time, live time, irradiation time, and cooling time respectively.

The neutron flux (Φ) calculated from Eq. (1) are given in Tables 3 and 4. From the photo-peak activity of γ-ray of ^{233}Pa and ^{239}Np, the ^{232}Th(n, γ) and ^{238}U(n, γ) reaction cross-sections (σ_R) were calculated by using the rearranged Eq. (2),

$$\sigma_R = \frac{A_{obs}\frac{CL}{LT}\lambda}{NI_\gamma \varepsilon\Phi(1-e^{-\lambda T_i})e^{-\lambda T_c}(1-e^{-\lambda CL})} \tag{2}$$

All the terms in Eq. (2) has the same meaning as in Eq. (1). The neutron flux (Φ) from Tables 3 and 4 were used in Eq. (2) to calculate the ^{232}Th(n, γ) and ^{238}U(n, γ) reaction cross-sections. The nuclear spectroscopic data were taken from literature (NuDat).

In the ^{232}Th(n, γ) and ^{238}U(n, γ) reactions, the cross-section values thus determined include the contribution from the low energy tail part. The contribution from the tail part has to be removed from the measured cross-sections. This contribution of the cross-section for the ^{232}Th (n, γ) and ^{238}U(n, γ) reactions have been estimated by calculating the weighted average values from ENDF/B-VII.1 and JENDL-4.0 (ENDF/B-VII.1, 2011; Shibata et al., 2011) by folding the cross-sections with neutron flux distributions taken from (Makwana et al., 2017). A similar approach was followed by other authors (Naik et al., 2011, 2012; Prajapati et al., 2012; Makwana et al., 2017).

3.2. Co-variance analysis

In the present measurement, we have used ^{232}Th(n, f)^{97}Zr reaction cross-sections for the measurement of flux for both the sample reactions. We have done the off-line gamma-ray spectroscopic measurement for both the sample reactions using a single pre-calibrated HPGe detector. Therefore, in the present work, both the sample reaction cross-sections are correlated with each other as well as among the four neutron energies. In such a case, covariance analysis can be used to find the degree of uncertainty in the measurement along with the correlation coefficients.

In the present case, the ratio measurement technique (Shivashankar et al., 2015) was used to normalize the measured cross-sections with monitor reaction cross-sections. We have adopted the method presented in Refs. (Shivashankar et al., 2015; Otuka et al., 2017). However, the micro correlation matrices S_{ijr}'s for the present case were modified keeping in mind the correlations among the quantities used in the calculations. The HPGe detector was calibrated using a point source, and the samples were of a finite size and hence they produce a geometry effect on the measured efficiencies of the detector. To incorporate the solid angle effect, the geometry and summing correction factors have been taken into account using the EFFTRAN code (Vidmar et al., 2011). The covariance matrix (V_{ij}'s) along with the correlation coefficients for the efficiencies and measured cross-sections for monitor and sample reactions are given in Tables 5 and 6, respectively. A detailed description of the method is also provided in our other recent publication (Parashari et al., 2018). The error in the measured cross-section can now be calculated as the product of tailing corrected cross-section with the square root of the diagonal element of the respective neutron energy ($\sqrt{V_{ii}} \times \sigma_R$) of the covariance matrix V_{ij}. The correlation coefficients for the measured cross-sections are given in Table 7. We have divided the table in four quadrants to make it more understandable. The first and fourth quadrant gives the correlations for the ^{232}Th(n, γ) and ^{238}U(n, γ) reaction cross-sections among the four neutron energies respectively. The third quadrant gives the correlations of ^{232}Th(n, γ) reaction cross-sections with ^{238}U(n, γ) reaction cross-sections among the four neutron energies. From the Table 7, it can be observed that the correlations are weakest among the monitor and the ^{238}U(n, γ) reaction cross-sections and strongest (diagonal elements in the third quadrant) among the two sample reactions, which is a result of using Th foils as monitor and sample calculations. The stated reason is also responsible for the significant correlations in the first quadrant, which are more than those given in fourth. The uncertainties thus calculated are given with the measured cross-sections for the present work in Tables 3 and 4.

Table 5
Covariance matrix for efficiencies used in the measurement.

γ-ray energy (keV)	Covariance matrix			Correlation coefficients		
277.6	1.45E-06			1		
311.26	1.41E-06	1.48E-06		0.960	1	
743.36	−1.1E-08	− 3.5E-08	5.86E-08	−0.039	−0.118	1

4. Results and discussion

The tailing corrected experimental cross section of ^{232}Th(n, γ) and ^{238}U(n, γ) reactions were determined after removing the contribution from the tail part of the neutron spectra as given in the Tables 3 and 4,

Table 4
The ^{238}U(n, γ) reaction cross-section at different neutron energy.

Neutron energy (MeV)	^{97}Zr Fission yields (%)	Spectrum averaged cross-section for Th monitor (mb)	Flux (n/cm^2.sec)	$^{238}_{92}U(n,\gamma)$ reaction cross section (mb)			
				Present work (mb)	TALYS-1.9 (mb)	ENDF (mb)	JENDL (mb)
5.08 ± 0.17	4.639 ± 0.42 (Naik et al., 2016)	99.0	1.06E+06	1.87 ± 0.34	2.91	2.080	1.159
8.96 ± 0.77	4.838 ± 0.35 (Naik et al., 2016)	220.0	4.2E+06	1.17 ± 0.16	1.00	0.653	1.096
12.47 ± 0.83	4.672 ± 0.33 (Naik et al., 2016)	270.0	1.11E+07	1.88 ± 0.31	1.50	1.021	0.776
16.63 ± 0.95	3.41 ± 0.15 (Mukerji et al., 2014)	342.0	1.11E+07	0.75 ± 0.10	0.737	0.455	0.313

Table 6
Covariance matrix for the measured cross-sections.

En (MeV)	Reaction	Covariance matrix							
5.08 ± 0.17	**Th (n, γ)**	0.027033							
8.96 ± 0.77		0.003553	0.021786						
12.47 ± 0.83		0.003553	0.003553	0.038442					
16.63 ± 0.95		0.003553	0.003553	0.003553	0.025693				
5.08 ± 0.17	**U (n, γ)**	0.016901	0.002464	0.002464	0.002464	0.034921			
8.96 ± 0.77		0.002464	0.010303	0.002464	0.002464	0.001974	0.018471		
12.47 ± 0.83		0.002464	0.002464	0.015266	0.002464	0.001973	0.001976	0.027509	
16.63 ± 0.95		0.002464	0.002464	0.002464	0.010833	0.001973	0.001976	0.001974	0.018328

respectively. The uncertainties associated with the measured ^{232}Th(n, γ) and ^{238}U(n, γ) reaction cross-sections were calculated using the covariance analysis. As mentioned before in the introduction, below the neutron energy of 3 MeV and within 13–15 MeV, there exists some literature data for the ^{232}Th(n, γ) (Perkin et al., 1958; Karamanis et al., 2001; Naik et al., 2011; Prajapati et al., 2012) and ^{238}U(n, γ) (Linenberger et al., 1944; Linenberger et al., 1946; Leipunskiy et al., 1958; Barry et al., 1964; Drake et al., 1971; Panitkin and Tolstikov, 1972a, 1972b; Poenitz, 1975; HuangZheng-De et al., 1980; Naik et al., 2012) reactions. In view of this, the present experimental and literature data within the neutron energies of 1–20 MeV are plotted in Figs. 4 and 5. The data reported by (Linenberger et al., 1946; Leipunskiy et al., 1958; Barry et al., 1964; Drake et al., 1971; Panitkin and Tolstikov, 1972a, 1972b) within the neutron energies of 5–7 MeV and 17–20 MeV as well as by (Perkin et al., 1958) at 14.5 MeV are significantly higher than the present data. On the other hand, the data of (McDaniels et al., 1982) around the neutron energies of 9.2–14.2 MeV are lower than the data of present work at the neutron energies of 8.96 ± 0.77, 12.47 ± 0.83 and 16.63 ± 0.95 MeV. The ^{238}U(n, γ) reaction cross-sections obtained by (Panitkin and Tolstikov, 1972a, 1972b) within the neutron energies of 5–7 MeV and 17–20 MeV as well as by (Perkin et al., 1958) at 14 MeV are based on the D + D and D + T neutron sources. In spite of this, the higher ^{238}U(n, γ) reaction cross-sections obtained by (Perkin et al., 1958) and (Panitkin and Tolstikov, 1972a, 1972b) are due to the contributions from the scattered low energy neutrons.

In order to examine these aspects, the ^{232}Th(n, γ) and ^{238}U(n, γ) reaction cross-sections within neutron energies of 1–20 MeV were also calculated theoretically by using the computer code TALYS-1.9 (Koning et al., 2015) with default parameters. The computer code TALYS-1.9 (Koning et al., 2015) is generally used for the prediction and analysis of nuclear reactions. TALYS-1.9 has two primary purposes; it can be used as a nuclear physics tool, confronting nuclear models with experiment and secondly, as a tool for the prediction of the nuclear data. The TALYS-1.9 program simulates nuclear reactions that involve gammas, neutrons, protons, deuterons, tritons, ^{3}He and alpha-particles in the incident energy range from 1 keV to 200 MeV for target nuclides of mass 12 and heavier. In the present work, we have used neutron energies up to 20 MeV for the irradiation of ^{232}Th and ^{238}U targets. All possible outgoing channels for a given projectile (neutron) energy were also considered including inelastic and fission channels. However, the cross-sections for the (n, γ) reactions were especially looked for and

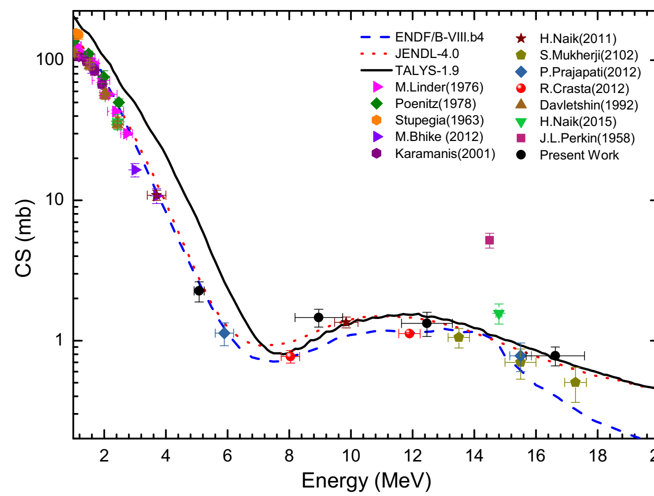

Fig. 4. Comparison of present experimental ^{232}Th(n, γ) reaction cross-section with the literature data, theoretical values from TALYS-1.9 and evaluated data of ENDF/B-VII.1 and JENDL-4.0.

collected. Theoretically calculated ^{232}Th(n, γ) and ^{238}U(n, γ) reaction cross-sections from neutron energy of 1–20 MeV using TALYS-1.9 are also plotted in Figs. 4 and 5. Besides this, the evaluated ^{232}Th(n, γ) and ^{238}U(n, γ) reaction cross-sections from the ENDF/B-VII.1 (ENDF/B-VII.1, 2011) and JENDL-4.0 (Shibata et al., 2011) nuclear data libraries are also shown in the respective figures.

In Figs. 4 and 5, it can be seen that the data from the present work follows the trend of theoretical values from TALYS-1.9 (Koning et al., 2015) and the evaluated data (ENDF/B-VII.1, 2011; Shibata et al., 2011). Further, it can also be observed that the theoretical (Koning et al., 2015), the evaluated (ENDF/B-VII.1, 2011; Shibata et al., 2011) and the experimental ^{232}Th(n, γ) and ^{238}U(n, γ) reactions cross-sections from the present work and literature (Perkin et al., 1958; Hanna and Rose, 1959; Stupegia et al., 1963; Lindner et al., 1976; Poenitz and Smith, 1978; Davletshin et al., 1992; Karamanis et al., 2001; Naik et al., 2011, 2015; Mukerji et al., 2012; Crasta et al., 2012; Prajapati et al., 2012; Bhike et al., 2012; Linenberger et al., 1944; Broda, 1945; Linenberger et al., 1946; Leipunskiy et al., 1958; Barry et al., 1964; Panitkin et al., 1971; Drake et al., 1971; Panitkin and Tolstikov, 1972a,

Table 7
Correlation matrix for the measured cross-sections.

En (MeV)	Reaction	Correlation matrix							
5.08 ± 0.17	Th (n, γ)	1.000							
8.96 ± 0.77		0.146	1.000						
12.47 ± 0.83		0.110	0.123	1.000					
16.63 ± 0.95		0.135	0.150	0.113	1.000				
5.08 ± 0.17	U (n, γ)	0.550	0.089	0.067	0.082	1.000			
8.96 ± 0.77		0.110	0.514	0.092	0.113	0.078	1.000		
12.47 ± 0.83		0.090	0.101	0.469	0.093	0.064	0.088	1.000	
16.63 ± 0.95		0.111	0.123	0.093	0.499	0.078	0.107	0.088	1.000

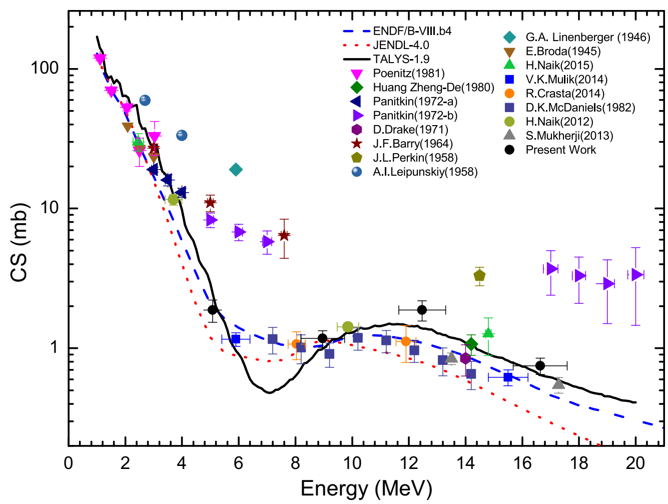

Fig. 5. Comparison of present experimental ^{238}U(n, γ) reaction cross-section with the literature data, theoretical values from TALYS-1.9 and evaluated data of ENDF/B-VII.1 and JENDL-4.0.

1972b; Poenitz, 1975; HuangZheng-De et al., 1980; McDaniels et al., 1982; Naik et al., 2012; Mukerji et al., 2013; Crasta et al., 2014; Mulik et al., 2014) decrease from the neutron energy 0.025 eV to 6–7 MeV. Thereafter, the (n, γ) reaction cross-section in both the reactions increase up to 12 MeV and then decrease. This is because at the neutron energy of 6.5 MeV the (n, 2 n) reaction of ^{232}Th and ^{238}U start increasing due to their threshold value of 6.47 MeV and 6.18 MeV, respectively. Below the 6 MeV neutron energies, there is a competition between (n, γ) and (n, n′) reaction cross-sections. The (n, n′) reaction cross-sections are larger by order of three than the (n, γ) reaction cross-sections in this energy regime. Furthermore, as (n, n′) reaction cross-section becomes almost constant beyond 7 MeV, then the (n, γ) and (n, 2 n) reactions start competing. On the other hand, as the ^{232}Th(n, 2 n) and ^{238}U(n, 2 n) reaction cross-sections start to increase, the ^{232}Th(n, γ) and ^{238}U(n, γ) reaction cross-sections decrease around the neutron energy of 6.5–7.5 MeV. When the (n, 2 n) reaction cross-section remains almost constant within 8–12 MeV, the (n, γ) reaction cross-section again increases. Above the neutron energy of 12–14 MeV, both the (n, γ) and (n, 2 n) reaction cross-sections decrease due to the opening of (n,3 n) reaction, which start at 11.33 MeV for ^{238}U and 11.61 MeV for ^{232}Th. Thus the different increase and decrease trend in the (n, γ) and (n, 2 n) reaction cross-sections are due to the sharing of energy.

5. Conclusions

The ^{232}Th(n, γ) and ^{238}U(n, γ) reactions cross-sections at the average neutron energies of 5.08 ± 0.17, 8.96 ± 0.77, 12.47 ± 0.83 and 16.63 ± 0.95 MeV have been experimentally determined by using the activation and off-line γ-ray spectrometric technique. The uncertainties in the measured quantities were calculated using the covariance analysis, which is a well-known error propagation method in nuclear data and was found to be in the range of 13–20%. The ^{232}Th(n, γ) and ^{238}U(n, γ) reactions cross-sections were compared with the TALYS-1.9 code, the evaluated data from ENDF/B-VII-1 and JENDL-4.0 nuclear data libraries and were found in consensus. The measured cross-section for both the ^{232}Th(n, γ) and ^{238}U(n, γ) reactions would be significant from the perspective of modern nuclear reactor technology; reactor generated waste transmutation and for the advancement of the present reactor technology.

Acknowledgments

One of the authors (SM) thanks to DAE-BRNS for the sanction of a major research project (Sanction number: 36(6)/14/22/2016-BRNS). The authors are thankful to the staff of TIFR-BARC Pelletron facility for their kind cooperation and help to provide the proton beam to carry out the experiment. They are also grateful to the staff of the target laboratory of Pelletron facility at TIFR, Mumbai, for providing us with Li and Ta foils. The author (VV) gratefully acknowledges the support given by the Maharaja Sayajirao University of Baroda, Vadodara.

References

Barry, J.F., Bunce, J., White, P.H., 1964. J. Nucl. Energy AB React. Sci. Technol. 18, 481.

Bhike, M., Roy, B.J., Saxena, A., Ganesan, S., 2012. Measurement of ^{232}Th(n,σ)^{233}Th, ^{98}Mo(n,σ)^{99}Mo, ^{186}W(n,σ)^{187}W, ^{115}In(n,σ)^{116m}1In, and ^{92}Mo (n,p)^{92m}Nb Cross Sections in the Energy Range of 1.6 to 3.7 MeV. Nucl. Sci. Eng. 170, 44.

Bowman, C.D., 1998. Accelerator-driven systems for nuclear waste transmutation. Annu. Rev. Nucl. Part. Sci. 48, 505.

Broda, E., 1945. Cavendish Lab. Reports No.574.

Crasta, R., Naik, H., Suryanarayana, S.V., Shivashankar, B.S., Mulik, V.K., Prajapati, P.M., Sanjeev, G., Sharma, S.C., Bhagwat, P.V., Mohanty, A.K., Ganesan, S., Goswami, A., 2012. Measurement of the ^{232}Th (n, γ) ^{233}Th and ^{232}Th (n, 2n) ^{231}Th reaction cross-sections at neutron energies of 8.04 ± 0.30 and 11.90 ± 0.35 MeV. Ann. Nucl. Energy 47 (2012), 160.

Crasta, R., Ganesh, S., Naik, H., Goswami, A., Suryanarayana, S.V., Sharma, S.C., Bhagwat, P.V., Shivashankar, B.S., Mulik, V.K., Prajapati, P.M., 2014. Measurement of the ^{238}U(n,γ)^{239}U and ^{238}U(n,2n)^{237}U reaction cross sections using a neutron activation technique at neutron energies of 8.04 and 11.90 MeV. Nucl. Sci. Eng. 178 (2014), 66–75.

Drake, D., Bergqvist, I., Mcdaniels, D.K., 1971. Dependence of 14 MeV radiative neutron capture on mass number. Phys. Lett. B 36, 557.

Davletshin, A.N., Teplov, E.V., Tipunkov, A.O., Tolstikov, V.A., Korzh, I.A., Ovdienko, V.D., Pravdivyy, N.M., Sklyar, N.T., Mishchenko, V.A., Davletshin, A.N., 1992. Vop. At. Nauki i Tekhn. Ser. Yad. Konstant. 41.

ENDF/B-VII.1, National Nuclear Data Center, Brookhaven National Laboratory, 2011. 〈http://www.nndc.bnl.gov/exfor/endf00.jsp〉.

Hanna, R.C., Rose, B., 1959. Fast neutron capture in ^{238}U and ^{232}Th. J. Nucl. Energy 8 (4), 197–205.

HuangZheng-De, Cao Zhong, Hui-Zhu, Wang, Ji-Shi, Liu, Da-Zhao, Ding, 1980. Lawrence Berkeley Lab. 243 (Reports No.11118).

IAEA-TECDOC-1319, 2002. Fast Reactors and Accelerator Driven Systems Knowledge Base, Thorium fuel utilization: Options and Trends.

Karamanis, D., Petit, M., Andriamonje, S., Barreau, G., Bercion, M., Billebaud, A., Blank, B., Chajkowski, S., Lacoste, V., Marchand, C., DelMoral, R., Giovinazzo, J., Perrot, L., Pravikoff, M., Tomas, J.C., 2001. Neutron Radiative Capture Cross Section of ^{232}Th in the Energy Range from 0.06 to 2 MeV. Nucl. Sci. Eng. 139, 282.

Koning, A.J., Hilaire, S., Goriely, S., 2015. TALYS User Manual: A Nuclear Reaction Program. NRG, ZG PETTEN, The Netherlands, pp. 1755.

Leipunskiy, A.I., Kazachkovskiy, O.D., Artyukhov, G.J., Baryshnikov, A.I., Belanova, T.S., Galkov, V.I., Stavisskiy, Yu.Ja., Stumbur, E.A., Sherman, L.E., 1958. Second Internat. At. En. Conference, Geneva, vol.15, p. 50.

Lindner, M., Nagle, R.J., Landrum, J.H., 1976. Neutron capture cross sections from 0.1 to 3 MeV by activation measurements. Nucl. Sci. Eng. 59, 381.

Linenberger, G.A., Miskel, J., Segre, E., Bailey, C., Blair, J., Frisch, D., Greene, D., Greisen, K., Hanson, A.O., Hush, J., Klema, E., Krohn, R., Perry, R., Seagondollar, W., Smith, W.D., Taschek, R., Turner, C., 1944. Los Alamos Scientific Lab. Reports No.137.

Linenberger, G.A. Miskel, J.A. Capture cross sections of several substances for neutrons at various energies. Los Alamos Scientific Lab. Reports, No.467 (1946).

Makwana, R., Mukherjee, S., Mishra, P., Naik, H., Singh, N.L., Mehta, M., Katovsky, K., Suryanarayana, S.V., Vansola, V., Sheela, Y.S., Karkera, M., Acharya, R., Khirwadkar, S., 2017. Measurements of the cross sections of the ^{186}W(n,γ)^{187}W, ^{182}W(n,p)^{182}Ta, ^{154}Gd(n,2n)^{153}Gd, and ^{160}Gd(n,2n)^{159}Gd reactions at neutron energies of 5 to 17 MeV. Phys. Rev. C 96, 024608.

McDaniels, D.K., Varghese, P., Drake, D.M., Arthur, E., Lindholm, A., Bergqvist, I., Krumlinde, J., 1982. Radiative capture of fast neutrons by ^{165}Ho and ^{238}U. Nucl. Phys. A 384, 88.

Mukerji, S., Naik, H., Suryanarayana, S.V., Chachara, S., Shivasankar, B.S., Mulik, V.K., Crasta, R., Samanta, S., Nayak, B.K., Saxena, A., Sharma, S.C., Bhagwat, P.V., Rasheed, K.K., Jindal, R.N., Ganesan, S., Mohanty, A.K., Goswami, A., Krishani, P.D., 2012. Measurement of ^{232}Th(n, γ) and ^{232}Th(n,2n) cross-sections at neutron energies of 13.5, 15.5 and 17.28 MeV using neutron activation techniques. Pramana 79 (2), 249.

Mukerji, S., Naik, H., Surayanarayana, S.V., Shivashankar, B.S., Mulik, V.K., Chachara, Sachin, Samanta, Sudipta, Goswami, A., Krishnani, P.D., 2013. Application of neutron activation techniques for the measurement of ^{238}U (n, γ) and ^{238}U (n, 2n) cross section at neutron energies of 13.5 and 17.28 MeV. J. Basic Appl. Phys. 2, 104.

Mukerji, S., Naik, H., Suryanarayana, S.V., 2014. In: Proceedings of the DAE Symposium on Nuclear Physics, vol. **59**, p. 426.

Mulik, V.K., Surayanarayana, S.V., Naik, H., Mukherji, Sadhana, Shivashankar, B.S., Prajapati, P.M., Dhole, S.D., Bhoraskar, V.N., Ganesan, S., Goswami, A., 2014. Measurement of the neutron capture cross-section of ^{238}U at neutron energies of 5.9 ± 0.5 and 15.5 ± 0.7 MeV by using the neutron activation technique. Ann. Nucl. Energy 63, 233.

Naik, H., Mukherji, S., Suryanarayana, S.V., Jagadeesan, K.C., Thakare, S.V., Sharma, S.C., 2016. Measurement of fission products yields in the quasi-mono-energetic

neutron-induced fission of ^{232}Th. Nucl. Phys. A 952, 100.
Naik, N., Surayanarayana, S.V., Bishnoi, S., Patel, T., Sinha, A., Goswami, A., 2015. Neutron induced reaction cross-section of ^{232}Th and ^{238}U at the neutron energies of 2.45 and 14.8 MeV. J. Radioanal. Nucl. Chem. 303, 2497.
Naik, H., Prajapati, P.M., Surayanarayana, S.V., Jagadeesan, K.C., Thakare, S.V., Raj, D., Mulik, V.K., Sivashankar, B.S., Nayak, B.K., Sharma, S.C., Mukherjee, S., Singh, S., Goswami, A., Ganesan, S., Manchanda, V.K., 2011. Measurement of the neutron capture cross-section of ^{232}Th using the neutron activation technique. Eur. Phys. J. A 47 (2011), 51.
Naik, H., Suryanarayana, S.V., Mulik, V.K., Prajapati, P.M., Shivashankar, B.S., Jagadeesan, K.C., Thakare, S.V., Raj, D., Sharma, S.C., Bhagwat, P.V., Dhole, S.D., Bhoraskar, V.N., Goswami, A., J., 2012. Measurement of the neutron capture cross-section of ^{238}U using the neutron activation technique. Radioanal. Nucl. Chem. 293, 469.
NuDat 2.7β, National Nuclear Data Center, Brookhaven National Laboratory. 〈http://www.nndc.bnl.gov/〉.
Otuka, N., Lalremruata, B., Khandaker, M.U., Usmand, A.R., Punte, L.R.M., 2017. Uncertainty propagation in activation cross section measurements. Radiat. Phys. Chem. 140, 502–510.
Panitkin, Yu.G., Stavisskiy, Yu., Ya., Tolstikov, V.A., 1971. Radiative capture of neutrons by U-238 in the energy range 0.024–1.1 MeV. Neutron Physics Conference, Kiev, vol. 1, p. 321.
Panitkin, Yu.G., Tolstikov, V.A., 1972a. Radiative capture of neutrons by U^{238} in the 1.2–4.0 MeV range. Sov. At. Energy 33, 893.
Panitkin, Yu.G., Tolstikov, V.A., 1972b. U^{238} radiative capture cross section for 5 to 20 MeV neutrons. Sov. At. Energy 33, 945.
Parashari, S., Mukherjee, S., Makwana, R., Singh, N.L., Singh, R.K., Naik, H., Suryanarayana, S.V., Nayak, B.K., Sharma, S.C., Mehta, M., Ayyala, S.A., Varmuza, J., Katovsky, K., 2018. Measurement of ^{100}Mo(n, 2n)^{99}Mo reaction cross-sections using 10–22 meV quasi-monoenergetic neutrons. In: Proceedings of the 19th International Scientific Conference on Electric Power Engineering (EPE), Brno, Czech Republic, pp. 1–5. 〈https://dx.doi.org/10.1109/EPE.2018.8395960〉.
Perkin, J.L., O`connor, L.P., Coleman, R.F., 1958. Radiative capture cross sections for 14.5 MeV neutrons. Proc. Phys. Soc. (Lond.) 72, 505.
Poenitz, W.P., Smith, D.L., 1978. Fast Neutron Radiative Capture Cross Section of ^{232}Th. Argonne National Laboratory Reports No. 42.
Poenitz, W.P., 1975. Measurements of the neutron Capture Cross Sections of Gold-197 and Uranium-238 between 20 and 3500 keV nuclear reactions ^{197}Au(n, γ), E = 400–3500 keV; ^{238}U(n, γ), E = 20–1200 keV; measured σ(E, Eγ). Nucl. Sci. Eng. 57, 300.
Prajapati, P.M., Naik, H., Suryanarayana, S.V., Mukherjee, Jagadeesan, S., Sharma, K.C., Thakre, S.C., Rasheed, S.V., Ganesan, K.K., Goswami, A, S., 2012. Measurement of the neutron capture cross-sections of 232Th at 5.9 MeV and 15.5 MeV. Eur. Phys. J. A 48, 35.
Rubbia, C., Rubio, J.A., Buono, S., Carminati, F., Fietier, N., Galvez, J., Geles, C., Kadi, Y., Klapisch, R., Mandrilion, P., Revol, J.P., Roche, C.H., 1995. Conceptual Design of a Fast Neutron Operated High Power Energy Amplifier, CERN Report No. CERN/AT/95-44 (ET).
Shibata, K., Iwamoto, O., Nakagawa, T., Iwamoto, N., Ichihara, A., Kunieda, S., Chiba, S., furutaka, K., Otuka, N., Ohasawa, T., Murata, T., Matsunobu, H., Zukeran, A., Kamada, S., 2011. JENDL-4.0: a new library for nuclear science and engineering. J. Nucl. Sci. Technol. 48.
Shivashankar, B.S., Ganesan, S., Naik, H., Suryanarayan, S.V., Nair, N.S., Prasad, K.M., 2015. Measurement and covariance analysis of reaction cross sections for ^{58}Ni (n,p)^{58}Co relative to cross section for formation of ^{97}Zr fission product in neutron-induced fission of ^{232}Th and ^{238}U at effective neutron energies En = 5.89, 10.11, and 15.87 MeV. Nucl. Sci. Eng. 179 (4), 423–433.
Stupegia, D.C., Smith, A.B., Hamm, K., 1963. Fast neutron capture in ^{232}Th. J. Inorg. Nucl. Chem. 25, 627.
Vidmar, T., Kanisch, G., Vidmar, G., 2011. Calculation of true coincidence summing corrections for extended sources with EFFTRAN. Appl. Radiat. Isot. 69 (6), 908–911.
Ziegler, J.F., 2004. Nucl. Instrum. Methods B 219, 1027. http://www.srim.org/.